



Fluid Dynamic Investigation of an Internal Circulating Fluidized Bed Gasifier by Cold Model

www.ericjournal.ait.ac.th

C. Freda*, G. Canneto*, P. Mariotti* G. Braccio*, E. Fanelli* and V.K. Sharma*¹

Abstract – Fluid dynamic behaviour of mineral bed and biomass particles in a steam/oxygen injected gasifier of thermal capacity 1 MW, having two interconnected fluidized chambers and investigated experimentally using a cold model, has been discussed in the present communication. It was ascertained that the architecture of reactor allows, using different fluidizing rates of gasifying agents in the two chambers, to the mineral particles to flow from the less fluidized chamber to the more fluidized one throughout the interconnection window at the bottom of the separating plate, and from the more fluidized chamber to the less one jumping the same plate. In this way the biomass particles despite of their lower density compared to the mineral bed are forced to sink in it, because of the flow direction of the sand particles. The distribution of biomass particles in the bed reactor results more uniform compared to a traditional fluidized bubbling bed reactor, so the elutriation phenomena of mineral and char fine particles is reduced with beneficial effect on the gasification yield, tar production, and gas cleaning.

Keywords – Fluidizing conditions, fluid dynamic investigation, gasifying agent, internal circulating fluidized bed gasifier, and mineral bed.

1. INTRODUCTION

Ever increasing energy demand, threats of climatic changes with billions of tonnes of carbon emissions into the atmosphere and the great obstacles to further development of conventional energy sources, it is very important that to achieve a sustainable energetic supply, due attention be given to a range of environmental-friendly renewable energy technologies. It is worth to note that amongst different renewable energy sources, biomass gasification is proving to be a consolidated technology for both thermal and electrical power generation. Substitution of fossil fuels by bio-energy, appears to be an effective strategy with the potential to meet 50% of world energy demands during the next century and at the same time meet the requirement of reducing carbon emissions from fossil fuels. It has been forecast that by 2050, 17 per cent of the world's electricity could be generated from modern biomass. Transforming wastes from agricultural, forest, and wood processing into gases using gasifier though complex still is a very efficient from an energetic point of view. Nowadays, searches concern the study of the renewable energy in agriculture with particular reference to the technologies for the energetic exploitation of the biomasses.

Gasification is a process that converts carbonaceous materials, such as coal, petroleum, or biomass, into carbon monoxide and hydrogen by reacting the raw material at high temperatures with a controlled amount of oxygen. The resulting gas mixture is called synthesis gas or syngas and is itself a fuel. However, relatively high contents of tar and fine particulate (that could seriously damage turbines and

internal combustion engines) are the main drawbacks of the syngas produced by gasification. It is true that the fine particulate content can efficiently be reduced using a cyclone and filter system but relatively high content of tar still remains a serious problem.

From the literature survey, it has been observed that amongst various reactors tested so far, it is the downdraft gasifier that produces syngas with lowest tar content (about 1 g/Nm³_{dry gas}). The bottleneck of this kind of reactor, however, remains its limited scalability up to 1.5 MW_{th}. On the contrary fluidized bed reactor can be used for commercial scale application up to 25 MW_{th}. Moreover, they have other advantages compared to the down-draft fixed bed such as good mixing and contact of the biomass particles with the bed material, uniformity of temperature in the reactor, quick starting and heating, possibility to use a wide range of biomass, etc. [1]. Unfortunately, the syngas produced by fluidized bed reactor has a medium tar content (about 10 g/Nm³_{dry gas}), high particulate content of mineral and carbonaceous nature. This can mainly be attributed to the fact that the biomass being less dense (compared to the mineral sand used as bed material) segregates on the top surface of bed reactor during the gasification. So, it is probable that the fine particles of sand and char leave the bed and are transported by the syngas.

This unwanted phenomenon can be reduced if the distribution of biomass particles in the mineral sand bed were more uniform and not limited to the top surface of the bed. This condition can be obtained by the circulation of bed material between different chambers. To resolve the above-cited problem, as shown in Figure 1, a few researchers used a reactor formed by four fluidized chambers separated by two orthogonal plates of different height and interconnected by two orifices at the bottom of higher plate [2]. By means of different fluidizing rates in the four chambers, it was possible to circulate the bed material from a less fluidized chamber

*ENEA Research Center Trisaia, 75026 Rotondella (MT), Italy.

¹Corresponding author; Tel: + 39 0835974220, Fax: + 39 0835974210
E-mail: sharma@trisaia.enea.it

to the more fluidized one throughout the orifice at the bottom of the higher plate and, vice versa, from a more fluidized chamber to the less fluidized chamber jumping the lower plate. It is in the above context that for the purpose of biomass gasification, a 500 kW_{th} thermal capacity steam injected Circulating Fluidized Bed Reactor (CFBR), having two fluidized beds (one for steam gasification and the other for the char combustion by air) was built at ENEA research centre Trisaia, in Southern Italy. The combustion supports the endothermic reactions in steam gasification. The energetic vector is the mineral bed material that flows from the combustor to the gasifier by means of different rate of fluidizing agents in two beds. So, it has two separated flows: one of syngas and other for exhaust combustion gas. By this arrangement, the syngas being not diluted of nitrogen in the air is benefited with increased heating value (13 MJ/Nm³) [3]. These advantages are balanced by drawbacks linked to the management of two flows. Moreover, the gasification of char to syngas is reduced by its circulation in the combustor. Also, an Internal Circulating Fluidized Bed Reactor (ICFBR) was considered for biomass gasification. Easy to manage and having only the syngas exit flow, ICFBR reactor is more advantageous compared to CFBR. To obtain a syngas with heating value comparable to that of syngas from the CFBR, a mix of steam and oxygen was proposed as a gasifying agent thus avoiding the dilution of syngas by the inert nitrogen of the air. As Figure 3 shows, ICFBR consists of a reactor divided into two interconnected chambers (through window at the bottom of the plate) by vertical plate. If the two chambers are differently fluidized, it will have two communicating beds with different density, so according to the hydraulic laws, mineral sand at the bottom window, will flow from the denser chamber to the less dense one. Moreover, if the height of mineral bed will be closer to the height of the separating plate, mineral particles (while jumping the separating plate), will flow from the less dense chamber to the denser one. In order to host the gaseous flux generated by the process and extend its residence time in the reactor, denser chamber section (from now onwards referred as down-flow chamber) increases with height. To avoid the formation of bad fluidized zone in the bed, which could influence negatively the whole process, wall is inclined at an angle of 60° with the horizontal, that is greater than the natural repose angle of the mineral sand (about 40°). By this arrangement, a continuous circulation of the mineral particles is guaranteed which determines, as said above, more uniform distribution of biomass particles in the reactor with increase of gasification yield, reduction of tar formation, reduction of fine particles of mineral and carbonaceous nature elutriated in syngas.

The fluid dynamic behaviour of the particles (sand and biomass) was investigated through cold model experimentation. Helpful information was obtained to support exercise on 1 MW_{th} plant (to build up in ENEA-Trisaia) where the segregation phenomena of biomass

on the top surface of the bed, is reduced compared to a traditional fluid bed reactor.

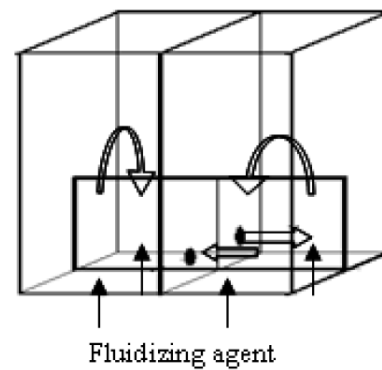


Fig. 1. Fluidized bed reactor with four interconnected chambers.

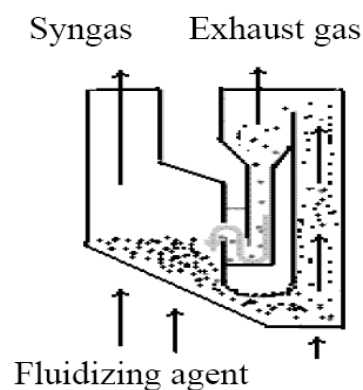


Fig. 2. 500 kW_{th} circulating fluid bed gasifier at ENEA Research Centre Trisaia.

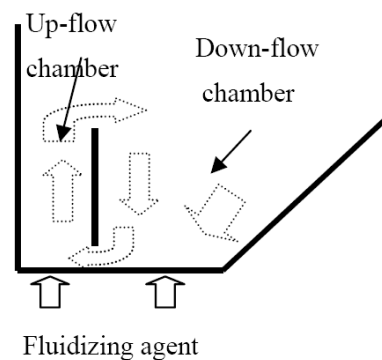


Fig. 3. Internal circulating fluidized bed gasifier.

2. BACKGROUND AND EXPERIMENTATION

The dynamic similitude is a powerful tool widely used to test and design fluidized bed reactor such as combustor or gasifier. In fact, it provides valid rules to build and test cold models at laboratory scale that in turn can easily be exercised for the prediction of fluid dynamic behaviour of a hypothetical fluid bed reactor. Scaling rules defined by more equations of heterogeneous fluidized system [4] were carefully validated experimentally [5]. Over the geometric similitude of reactor and of the solid particles present in it, the gasifier reactor and the cold model must have the same values of three dimensionless number (Archimedes number, gas density /solid density ratio number, and Froude number [6] :

$$De = \frac{\rho}{\rho_p} \quad (1)$$

$$Ar = \frac{d_p^3 \rho_p (\rho_p - \rho) g}{\mu^2} \quad (2)$$

$$Fr = \frac{U}{0.5(gL)} \quad (3)$$

In cold model experimentation, for logistic reason, it was decided to use fluidizing agent air at room temperature and one atmosphere pressure. Thus being aware of the design and operating condition of hot

gasifier (temperature, pressure, mineral sand and biomass particles properties), based upon the three dimensionless numbers, it was possible to determine the dimensions of the cold model, its particles properties and gas flow rates. The equality of the density ratio (equation 1) in the gasifier reactor with the cold model, fixes the density of the bed particles for the cold model while their diameter is fixed by the equality of Archimedes number (equation 2). The ratio between the particles diameter (in cold model) and gasifier reactor will help to fix the geometrical scale factor between the two systems.

Table 1. Operating condition of the gasifier and cold model (similitude criteria).

	Gasifier 800°C, 1 atm	Cold model 20°C, 1 atm
gas density (kg/m ³)	0.32	1.2
gas viscosity (Pa*s)	4*10 ⁻⁵	1.8*10 ⁻⁵
particles density (kg/m ³)	2400	9000
particle diameter (μm)	500	125
geometrical scale factor	4	1
gas rate factor	2	1
Vol. gas flow factor	32	1
time scale factor	2	1

Gas rate factor between the two systems is obtained from Froude Number (Equation 3) thus ensuring the dynamic similitude conditions. Results obtained with respect to the cold model while making use of the above-mentioned equations, are reported in Table 1. It is obvious from the results that it is possible to build a cold model with geometrical dimensions reduced by four times compared to the hot gasifier. Moreover, use of gas flow could be reduced by factor of 32 compared to the hot gasifier.

Furthermore as per definition of the cold model, it is important to consider that the fluidizing gas (steam and oxygen) in the gasifier reactor enter throughout the nozzles at about 500 °C while the operating conditions are maintained at about 800 °C. To maintain ratio of the momentum of gas (throughout the holes of distributor nozzles between gasifier and in the cold model) to be equal, the following conditions must be satisfied:

$$\left| \frac{S_{nozzle}}{S_{bed}} \right|_{cold\ model} = \left| \frac{S_{nozzle} \rho_{g(nozzle)}}{S_{bed} \rho_{g.bed}} \right|_{gasifier} \quad (4)$$

This means that the diameter of the holes in cold model has to be greater than that of the calculated one using geometrical similitude.

In accordance with the results obtained from similitude criteria (Table1) it was thought to simulate the copper powder as bed material (Table 2). With moderated bed expansion and minimum bubbling rate just a little above than the minimal fluidization one, it belongs to group B of Geldart classification [7]. About

60 kg of copper powder were filled in the cold model. The height of the bed under minimal fluidizing condition was about 28 cm; approximately equal to that of the separating plate. The biomass particles fed to the gasifier were simulated in the cold model using spherical glass particles of diameter consistent with the geometrical scale factor and density consistent with the density ratio of biomass and the bed particles in the gasifier (Table 2).

Table 2. Material used in the cold model.

	Copper powder	glass spheres
D _p (μm)	122	2200
ρ _p (kg/m ³)	8822	2600
U _{mf} (cm/s)	5.5	
ε _{mf}	0.4	

To observe the tests carefully, cold model was realized in Plexiglas. The design of this model was very similar to that of the gasifier reactor (Figure 4). The gas was distributed by seven outlets at the bottom of the model (everyone having six holes) and to avoid the formation of bed fluidized zones, four outlets were placed along the sloping wall. The volumetric flow rate was measured by rotameter calibrated at 1 bar and 25 °C. The main objective of the tests conducted are given below:

- To measure pressure drop in the bed particles of low density chamber (from now onwards referred as up-flow chamber) using a metallic probe of

internal diameter 6 mm and centrally sunk about 7 cm in the bed) connected to a U tube manometer filled by water. In order to determine the minimum fluidizing rate, fluidizing condition were varied.

- To measure pressure difference (caused by different fluidizing conditions) at the bottom of the two chambers. In the process, the probes were sunk centrally in every chamber down to 1.5 cm from the bottom of the reactor).
- Recirculation test of glass spheres in the two chambers at different fluidizing condition; simultaneously, feeding the down-flowing chamber with one hundred glass spheres and measuring the time the sphere spend to pass from down flow chamber to the up flow chamber through an interconnected lower window and to move from up flow chamber to down flow chamber while jumping over the separating plate. When the spheres returned in the down flow chamber, a metallic holed basket, welded to separating plate, stopped their run, without interfering with the fluidizing phenomena.
- To measure time required for jumping of twenty spheres over the separating plate from the bottom of the up-flow chamber to the down-flow chamber for different fluidizing condition, in the two chambers. Also, in these tests, a metallic holed basket was used to stop the spheres.
- To conduct re-circulation tests for one hundred spheres, at various height of the bottom window (from 3 cm to 7 cm), fixing the fluidization conditions in the chambers.

3. RESULTS AND DISCUSSION

The minimal fluidization rate in the up-flow chamber was determined by pressure drop measurement in the bed as a function of the fluidization gas flow rate

(increasing and decreasing). The results, with minimal fluidization value of 5.5 cm/s, are presented in Figure 5. Under such condition, pressure drop along the bed becomes equal to weight of the bed divided the section area. The minimal fluidization rate calculated theoretically (using Ergun's formula, equation 5) resulted to be 4.9 cm/s. The difference could probably be attributed, to the system's geometrical difference used by Ergun.

$$g(\rho_s - \rho_g)(1 - \varepsilon_{mf}) = 150\mu_{mf} \frac{(1 - \varepsilon_{mf})^2}{d_{mf}^2 \varepsilon_{mf}^3} + \frac{1.75\rho_g u_{mf}^2 (1 - \varepsilon_{mf})}{d_{mf} \varepsilon_{mf}^3} \quad (5)$$

From here onward, fluidizing condition of the bed, will be referred as the dimensionless number U/U_{mf} . The driving force of bed material circulation between the reactor chambers is the difference in bed density of two chambers thus generating different pressures at the same height. Measures of pressure drop were executed between the chambers at 1.5 cm from the bottom of the reactor (approx. at the middle of bottom window) with fluidization rate in the down-flow chamber equal to 1.5 and 1.7 U_{mf} , whereas the fluidization rate in the up-flow chamber varying between 1.5 to 4 U_{mf} (Figure 6). As expected, the highest pressure drop was observed at the highest fluidizing rate in the up-flow chamber whereas in the down-flow chamber it occurred the lowest fluidizing rate. The transition from a regular bubbling regime to a slugging regime was observed in the up-flow chamber at about 4 U_{mf} . This regime occurs at mean bubble diameter equal to minor dimension of the chamber, in other words this regime causes elutriation of both bed and biomass particles.

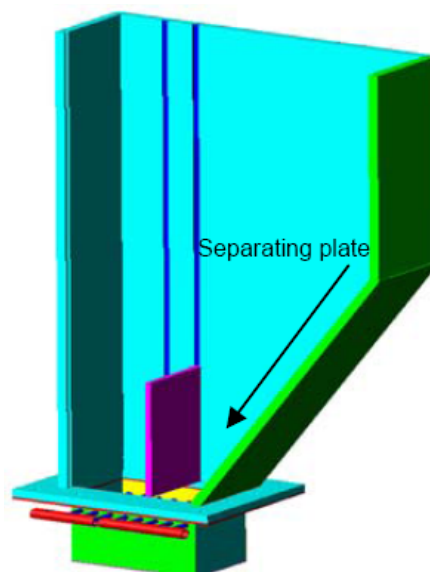


Fig. 4. Sketch of Plexiglas Cold Model

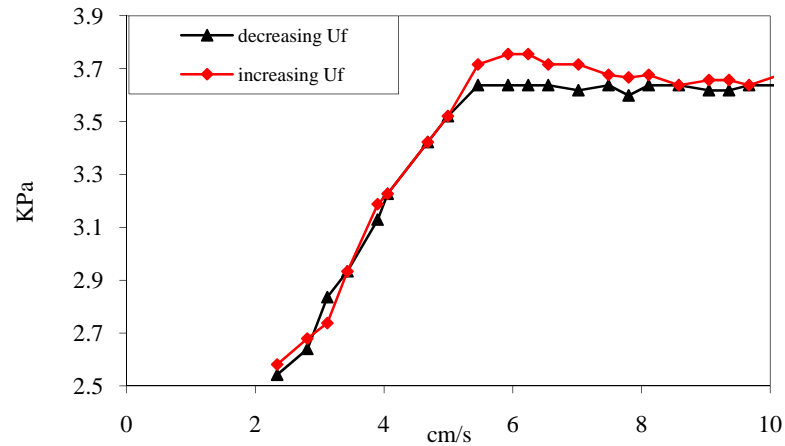


Fig. 5. Pressure drop in the up-flow chamber as a function of fluidizing rate.

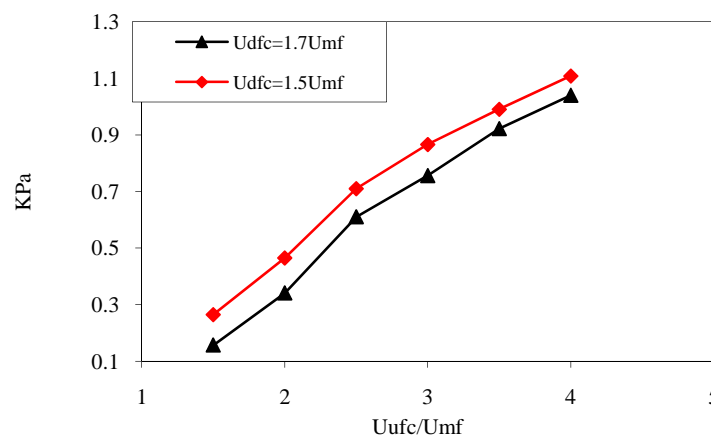


Fig. 6. Pressure drop at the bottom of the chambers as a function of fluidizing rate ($\blacklozenge U_{dfc}/U_{mf} = 1.5$, $\blacktriangle U_{dfc}/U_{mf} = 1.7$).

The theoretical diameter of the bubble, as given below, was calculated according the Darton *et al.* formula [8]:

$$d_b = 0.54(U - U_{mf})^{0.4} (h + 4\sqrt{A_d})^{0.8} g^{-0.2} \quad (6)$$

and near the top of bed ($= 7$ cm), that is, value equal to the minor dimension of chamber, it resulted at U_{ufc} equal to $4 U_{mf}$. However, to avoid this situation, re-circulation tests were conducted at a fluidizing condition in the up-flow chamber less than $4 U_{mf}$. The results obtained at fixed U_{dfc} equal to $1.7 U_{mf}$, but varying U_{ufc} from 2 to $3.5 U_{mf}$, are presented in Figure 7. From the data reported in Table 3, it can be observed that at $U_{ufc} = 2 U_{mf}$ and a relatively long time of about 4 hours, re-circulated fraction of glass spheres is about 65% whereas the remaining fraction of the spheres did not re-circulate even after long fluxing period of 8 hours or so. This could probably be attributed to the similar fluidizing conditions in the two chambers. Furthermore, boiling phenomena observed in the down-flow chamber area helped spheres to get stationed into the bed fluidized zones until the fluidization condition were improved. Increased fluidizing conditions in the up-flow chamber (up to $2.5 U_{mf}$) results into faster re-circulation rate, i.e.

93% in just 1.6 hours. More fast and better recirculation (95% in just an hour) was observed with further enhancement of fluidizing condition in the up-flow chamber ($= 3 U_{mf}$). It is obvious from the results obtained that optimum recirculation of spheres both in term of percentage and time (97 % in just 0.58 hour) was achieved when fluidizing condition in the up-flow chamber were equal to $3.5 U_{mf}$. So, based upon the data, it can be concluded that because of the higher pressure drop at the bottom window of separating plate, an increase of fluidizing condition in the up-flow chamber on one hand when helps to increase the re-circulated fractions at the same time decreases the recirculation period, significantly.

The above-mentioned tests were also conducted with recirculation time, $U_{dfc} = 1.5 U_{mf}$ with fluidizing conditions, U_{ufc} , varying between 2 to $3.5 U_{mf}$ (Figure 8). In the above tests with U_{ufc} equal to 2 and $2.5 U_{mf}$, unsatisfactory recirculation fractions of 36% and 78%, were observed. However, by increasing the U_{ufc} value to 3 and $3.5 U_{mf}$, re-circulation fractions increases up to 92 and 94 %, respectively, whereas the average re-circulation periods decreases further (Table 3).

During recirculation tests, it was observed that the spheres move chaotically up and down in the chambers. In particular, against their natural tendency to float on

top surface of the bed, they move towards the bottom of chamber driven by the particles flow in the down-flow chamber, until they meet a bubble that drags them towards the top. Here, they are submerged by bed particles fired from the bubble explosions generated in the same as well as in the up-flow chamber (whose fluidization condition is more vigorous).

The spheres repeat this chaotic path until they reach the bottom of the chamber at the depth of the bottom window, where pushed by the pressure drop between the two chamber, cross the window and get into the up-flow chamber. At this stage, because of their both lower density compared to the bed density and ascending path of the bubbles and bed particles, they are pushed towards the top surface of the bed.

Table 3. Average re-circulation periods (A.R.P.) and standard deviation (s.d.) for different fluidizing conditions in the two chambers.

U_{ufc}	A.R.P. \pm s.d. $U_{dfc} = 1.7 U_{mf}$ (s)	A.R.P. \pm s.d. $U_{dfc} = 1.5 U_{mf}$ (s)
$2 U_{mf}$	6376 ± 3551	10283 ± 5531
$2.5 U_{mf}$	2587 ± 1329	8460 ± 4567
$3 U_{mf}$	1782 ± 936	1086 ± 630
$3.5 U_{mf}$	1037 ± 547	679 ± 330

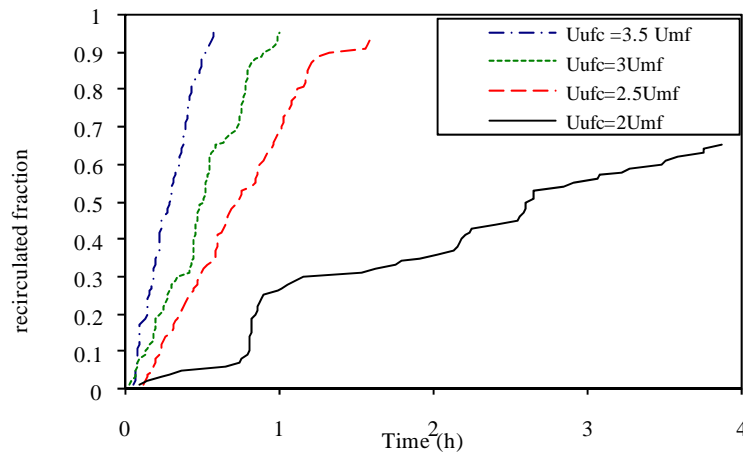


Fig. 7. Re-circulated fraction of spheres as function of time at U_{dfc} fixed = $1.7 U_{mf}$, but different fluidizing conditions in U_{ufc} .

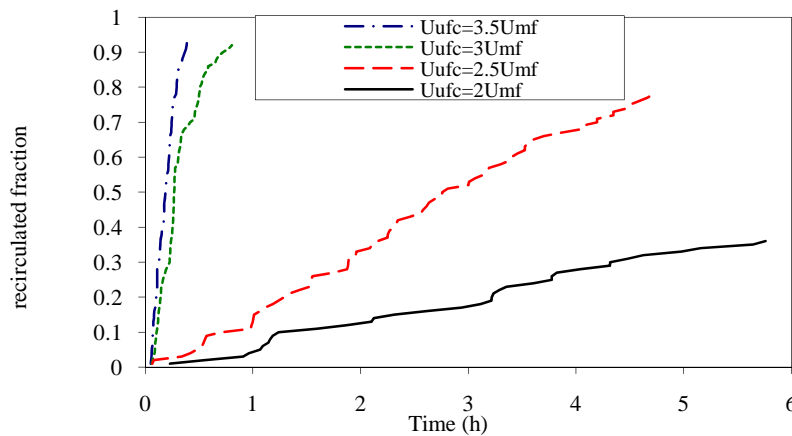


Fig. 8. Re-circulated fraction of spheres as function of time at U_{dfc} fixed = $1.5 U_{mf}$, but different fluidizing conditions in U_{ufc} .

Once reached at the top of the bed, spheres are pushed up by bubbles explosion. The sphere having enough energy and right direction, after jumping the separating plate of the chamber, once again, enters into the down-flow chamber. On the contrary, if the bubble explosion fails to provide right direction or the enough energy to jump the plate, the sphere gets submerged in the up-flow chamber by the bubble explosion. Pushed by

the bubbles and their floating tendency, in a relatively short time, they reach again at the top surface of the bed. It is because of this fact that the spheres spent majority of their time in the down-flow chamber. Instead, in the up-flow chamber their path is driven by concord forces towards the top of the bed. Measuring time that the spheres take to jump from the bottom of this chamber to the other, it was possible to quantify the time the spheres

spent in both the chambers. Data presented in Table 4 clearly shows that total jumped fraction (100 %) is possible for every test. The average jumping times (Table 4), significant lower compared to recirculation periods, confirms the above-discussed hypothesis of the spheres path in the cold model. It can be observed from Table 4 that the average jumping times when the U_{dfc} is equal to $1.5 U_{mf}$, are always superior compared to the values obtained when U_{dfc} is fixed at $1.7 U_{mf}$. This fact can probably be justified by higher amount of flux of the fluidizing agent from the up-flow chamber to the down flow, when U_{dfc} is equal to $1.5 U_{mf}$ compared to the case when U_{dfc} value is fixed at $1.7 U_{mf}$.

Finally, re-circulation tests were executed to evaluate the effect of the area of the bottom window of interconnecting the two chambers at different height but identical fluidizing conditions in the chambers ($U_{ufc} = 2.5 U_{mf}$, and $U_{dfc} = 1.7 U_{mf}$).

It is evident from the results presented in Figure 9 that with bottom window height increase from 3 cm to 7 cm, the re-circulated fraction increases from 92 to 100 %.

Moreover, as shown in Table 5, average re-circulation period decreases to 66 % with increase in bottom window height from 3 to 7 cm.

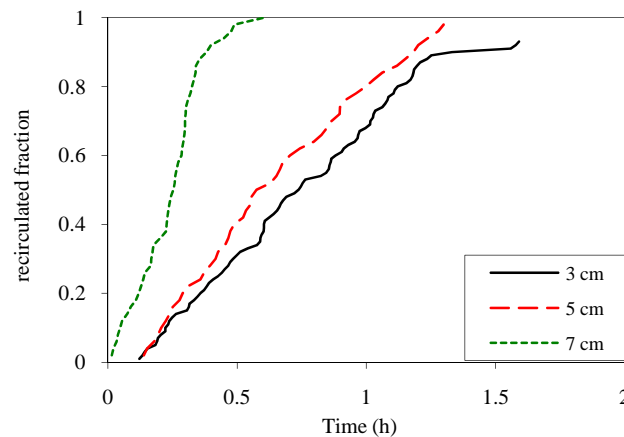


Fig. 9. Re-circulated fraction at $U_{ufc} = 2.5 U_{mf}$ and $U_{dfc} = 1.7 U_{mf}$ Vs time at different heights of the bottom window.

Table 4. Jumped fraction (J.F.), average jumping time (A.J.T.) and standard deviation (s.d.), for different fluidizing conditions in two chambers.

U_{ufc}	J.F. $U_{dfc} = 1.7 U_{mf}$ (%)	A.J.T. $U_{dfc} = 1.7 U_{mf}$ (s)	J.F. $U_{dfc} = 1.5 U_{mf}$ (%)	A.J.T. $U_{dfc} = 1.5 U_{mf}$ (s)
$2 U_{mf}$	100	57 ± 27	100	117 ± 42
$2.5 U_{mf}$	100	72 ± 40	100	146 ± 60
$3 U_{mf}$	100	83 ± 45	100	190 ± 91
$3.5 U_{mf}$	100	88 ± 41	100	172 ± 81

Table 5 Average re-circulation period (A.R.P.) and standard deviation (s.d.) at $U_{ufc} = 2.5 U_{mf}$ and $U_{dfc} = 1.7 U_{mf}$, for different heights of the bottom window.

Bottom window height (cm)	A.R.P. \pm s.d. (s)
3	2587 ± 1329
5	2327 ± 1233
7	869 ± 465

4. CONCLUSIONS

Following are the main conclusion drawn from the cold model testing of 1 MW_{th} steam-oxygen injected Internal Circulating Fluidized Bed Reactor for biomass gasification.

- Good fluidizing condition was observed in down-flow chamber with fixed U_{dfc} value, at least, equal to $1.5 U_{mf}$. Minor fluidizing condition generates bad fluidizing zones with spheres station therein.

On the other hand, U_{ufc} equal to $4 U_{mf}$, transition from bubbling to a slugging regime takes place, in the up-flow chamber.

- The recirculation tests, conducted with U_{dfc} values fixed at 1.5 and $1.7 U_{mf}$ while varying the U_{ufc} from 2 to $3.5 U_{mf}$, it has been observed that with U_{dfc} equal to $1.5 U_{mf}$, a satisfactory recirculation fraction of the order of 92 and 94%, was obtained for U_{ufc} values equal to 3 and $3.5 U_{mf}$, respectively.

In another test with U_{dfc} equal to $1.7 U_{mf}$, once again, satisfactory recirculation fraction of 93%, was obtained also for U_{ufc} equal to $2.5 U_{mf}$. As expected, if the pressure drop between the two chambers at the depth of the interconnection bottom window increases, the average recirculation periods decreases.

- The jumping tests of spheres from bottom of the up-flow chamber to the down-flow chamber show that the spheres spent majority of their time (up to 99 %) moving chaotically in the down-flow chamber but cross the up-flow chamber, very quickly.
- Increasing the height of the bottom window from 3 to 7 cm (fixing $U_{ufc} = 2.5 U_{mf}$ and $U_{dfc} = 1.7 U_{mf}$), recirculation fraction increase from 93 % up to 100 %, and average recirculation period decrease of 66%, was observed.
- Compared to a traditional fluid bed, there will be more efficient energetic exchange between the sand and biomass (because of the more uniform distribution of the biomass in the bed) with probable increase in the gasification yield, reduction of content of tar in syngas and elutriation of fine particulate of carbonaceous and mineral nature.

ACKNOWLEDGEMENT

The authors would like to express their sincere thanks to Mr. Bellino A., Mr. Battafarano A., Mr. Villani M., Mr. Petrocelli G., and Mr. Corrado M. for the technical support. Helpful discussion and valuable suggestion given by Mr. Jand N. from Università Dell'Aquila is duly acknowledged.

NOMENCLATURE

d	particles diameter
ρ	density
g	gravity acceleration
μ	viscosity
L	length
U	gas velocity
ε	bed void fraction
h	bed height
A_d	distributor plate area /number of holes
S	area

A.R.P.	average re-circulation period
s.d.	standard deviation
J.F.	jumped fraction
A.J.T.	average jumping time

Subscripts

p	particle
mf	minimal fluidization
g	gas
s	solid
dfc	down-flow chamber
ufc	up-flow chamber

REFERENCES

- [1] Bridgwater, A.V., 2003. Renewable fuels and chemicals by thermal processing of biomass. *Chemical Engineering Journal* 91: 87-102.
- [2] Kunii, D., and Kuramoto, M., 1985. Development of a new system for circulating fluidizing particles within a single vessel. *Powder Technology* 44: 77-84.
- [3] Fiorenza, G., Canonaco, J., Amelio, M., Braccio, G., and Zimbardi, F., 2007. Advanced model for biomass steam gasification processes. In *Proceedings of 15th European Biomass Conference & Exhibition*. Berlin, Germany, 7-11 May.
- [4] Foscolo, P.U., Di Felice, R., Gibilaro, L.G., Pistone, L., and Piccolo, V., 1990. Scaling relationships for fluidisation: the generalised particle bed model. *Chemical Engineering Science* 45: 1647-1651.
- [5] Di Felice, R., Rapagnà, S., and Foscolo, P.U., 1992. Dynamic similarity rules: validity check for bubbling and slugging fluidized beds. *Powder Technology* 71: 281-287.
- [6] Gibilaro, L.G., 2001. *Fluidization-Dynamics*. Oxford: Butterworth Heinemann.
- [7] Geldart, D., 1973. Types of gas fluidization. *Powder Technology* 7: 285-292.
- [8] Darton, R. C., La Nauze, R. D., Davison, J. F., and Harrison, D., 1977. Bubble growth due to coalescence in fluidized beds. *Trans. IChemE* 55: 274-280.